



**HAL**  
open science

## Oxidation of stoichiometric nickel ferrites used as inert anodes for aluminium electrolysis in molten cryolite mixtures

Laurent Cassayre, Pierre Chamelot, Laurent Arurault, Laurent Massot, Pierre Taxil

### ► To cite this version:

Laurent Cassayre, Pierre Chamelot, Laurent Arurault, Laurent Massot, Pierre Taxil. Oxidation of stoichiometric nickel ferrites used as inert anodes for aluminium electrolysis in molten cryolite mixtures. High-Temperature Corrosion and Protection of Materials Conference, May 2008, Îles des Embiez, France. pp.0. hal-04089021

**HAL Id: hal-04089021**

**<https://hal.science/hal-04089021>**

Submitted on 4 May 2023

**HAL** is a multi-disciplinary open access archive for the deposit and dissemination of scientific research documents, whether they are published or not. The documents may come from teaching and research institutions in France or abroad, or from public or private research centers.

L'archive ouverte pluridisciplinaire **HAL**, est destinée au dépôt et à la diffusion de documents scientifiques de niveau recherche, publiés ou non, émanant des établissements d'enseignement et de recherche français ou étrangers, des laboratoires publics ou privés.

# Oxidation of stoichiometric nickel ferrites used as inert anodes for aluminium electrolysis in molten cryolite mixtures

L. Cassayre<sup>1,a</sup>, P. Chamelot<sup>1,b</sup>, L. Arurault<sup>2,c</sup>, L. Massot<sup>1,d</sup>, and P. Taxil<sup>1,e</sup>

<sup>1</sup> Laboratoire de Génie Chimique (LGC) UMR CNRS 5503, Université Paul Sabatier, 31062 Toulouse Cedex 09, France

<sup>2</sup> Centre Interuniversitaire de Recherche et d'Ingénierie des Matériaux (CIRIMAT), UMR CNRS 5085, Université Paul Sabatier, 31062 Toulouse Cedex 09, France

<sup>a</sup> cassayre@chimie.ups-tlse.fr, <sup>b</sup> chamelot@chimie.ups-tlse.fr, <sup>c</sup> arurault@chimie.ups-tlse.fr,

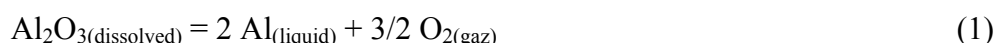
<sup>d</sup> massot@chimie.ups-tlse.fr, <sup>e</sup> taxil@chimie.ups-tlse.fr

**Keywords:** molten salts, cryolite, inert anode, aluminium production, nickel ferrite.

**Abstract.** Thanks to their good electronic conductivity and their low solubility in cryolite melts, nickel ferrites are considered to be among the most suitable ceramic materials that could be used as inert anodes in the electrowinning of aluminium. In this work, electrodes composed of single phased and stoichiometric nickel ferrite  $\text{Ni}_x\text{Fe}_{3-x}\text{O}_4$  ( $0 \leq x < 1$ ) have been studied by electrochemical techniques (linear voltammetry and potentiostatic electrolysis) in a molten cryolite mixture at 960°C. The aim was to understand the oxidation reactions susceptible to take place inside the material under anodic polarization and oxygen evolution. *Ex situ* characterization of the electrodes by SEM-EDX and microprobe analysis allows proposing a degradation mechanism of the pure nickel ferrites: the formation of haematite  $\text{Fe}_2\text{O}_3$  at the grain boundaries was evidenced and it resulted in a slow degradation. The influence of the Ni content in the ceramic phase was investigated, and it was shown that rich-Ni compositions exhibit a better resistance to corrosion.

## Introduction

One of the main actual stakes concerning the primary aluminium production is the development of a new inert anode material in place of the usual consumable carbon anode in order to achieve the following cell reaction:



This process would allow suppressing the massive amount of  $\text{CO}_2$  released at the carbon anode in the present Hall-Héroult cells and help reducing the world green-house gases emissions [1].

Among the required properties for the anode material, the stability under strong oxidative conditions (production of oxygen, at 1000°C, in a corrosive fluoride melt composed mainly of cryolite  $\text{Na}_3\text{AlF}_6$ ) is one of the most difficult to achieve. Many materials (metals, ceramic phases and ceramic-metal composites called cermets) have been developed for this application [2], but up to date none of them was found resistant enough against corrosion for a long term (about 2 years) industrial application.

Corrosion studies involving pure ceramic phases for a use as inert anodes are quite scarce. Among the studied materials are tin oxide electrodes ( $\text{SnO}_2$ ) [3-5], cobalt ferrites ( $\text{CoFe}_2\text{O}_4$ ) [6, 7] and more recently zinc ferrite ( $\text{ZnFe}_2\text{O}_4$ ) [8]. Thanks to their good electronic conductivity and their low solubility in cryolite melts, nickel ferrites are also considered to be among the most suitable ceramic materials [9].

In this work, electrodes composed of pure and stoichiometric nickel ferrite  $\text{Ni}_x\text{Fe}_{3-x}\text{O}_4$  ( $0 \leq x \leq 1$ ), elaborated under controlled conditions [10], have been studied by electrochemical techniques (linear voltammetry and potentiostatic electrolysis) in a molten cryolite mixture at  $960^\circ\text{C}$ . The aim was to understand the oxidation reactions susceptible to take place inside the material and which could provoke its deterioration under anodic polarization and oxygen evolution. Subsequent SEM-EDX characterization and microprobe analysis were performed on the cross-section of the electrodes in order to determine the corrosion products and propose a degradation mechanism.

## Experimental

**Cell.** The liquid cryolite mixture was contained in a vitreous carbon crucible, placed in a graphite liner protecting the inside wall of a cylindrical vessel made of refractory steel. The cell was closed by a stainless steel lid cooled by circulating water.

The atmosphere in the cell was composed of U-grade inert argon dehydrated with a purification cartridge (Air Liquide), containing less than 5 ppm of  $\text{O}_2$  and  $\text{H}_2\text{O}$ . An absolute pressure of 1.3 bars was maintained during the runs.

**Techniques and equipment.** Electrochemical measurements were carried out using an Autolab PGSTAT30 potentiostat controlled by GPES software. Two electrochemical techniques were used. Steady state current versus potential curves were recorded by applying a sweep rate of 0.01 V/s; short (30 min) electrolyses at fixed potential allowed to record the evolution of current with time. The electrodes were then cut, embedded in resin and polished for surface analysis of their cross-sections. Scanning electron microscope (SEM) observations were made on a LEO 435 VP. A microprobe CAMECA Sx100 was used for composition measurements.

**Electrolyte.** The mixture was composed of pure  $\text{Na}_3\text{AlF}_6$  (Cerac, purity 99.5%), with an 11 wt.% excess of  $\text{AlF}_3$  (Acros, purity 99.9+%) leading to a cryolite ratio (CR = molar ratio  $\text{NaF}/\text{AlF}_3$ ) of 2.2. In addition, 5 wt.% of  $\text{CaF}_2$  (Merck, purity 99.95%) and 9 wt.% of alumina were included. The liquidus temperature was calculated to be  $934^\circ\text{C}$  [11].

Two hundred grams of the mixture were placed in the cell, heated to  $500^\circ\text{C}$  and dehydrated under vacuum ( $10^{-5}$  bar) for 24 h. A temperature of  $25^\circ\text{C}$  above the melting point was maintained during electrochemical experiments, i.e.  $960^\circ\text{C}$ . At this temperature, the alumina solubility is 8.3 wt.% according to Skybakmoen *et al.* [12]; the melt was then saturated with alumina, with an excess of about 0.7 wt.%.

**Electrode materials.** A classic three-electrode set-up composed of a graphite auxiliary electrode, a nickel comparison electrode and a ceramic working electrode was used. The auxiliary electrode was an 8 mm diameter graphite rod (Carbone Lorraine). Potentials were measured with respect to a nickel wire (1 mm in diameter) protected by an insulating boron nitride cylinder drilled with a 0.2 mm hole at the bottom. The equilibrium potential of this comparison electrode was calibrated in regard of the oxygen evolution potential, determined by cyclic voltammetry on a platinum working electrode. It was found to be stable within  $\pm 10$  mV during the course of the electrochemical measurements, even under strong oxygen bubbling at the anode.

The working electrodes were made of nickel ferrite with a cylindrical shape (8 mm in diameter and 20 mm in height). The connexion to the inconel current lead was assured by a graphite holder protected by a copper foil to avoid any reaction between the graphite and the ceramic. The nickel ferrites rods were prepared by Corso *et al.* [10]. The elaboration of these semi-conducting ceramics was focused on obtaining single phased spinel with a stoichiometric O/metal ratio equal to 4/3. Six compositions (three rods per composition) were tested in this study. In each case, the composition

(noted as  $x$  in  $\text{Ni}_x\text{Fe}_{3-x}\text{O}_4$ ) was determined by microprobe analysis of Ni and Fe. The compositions are:  $x=0$  (pure  $\text{Fe}_3\text{O}_4$ );  $x=0.22$ ;  $x=0.48$ ;  $x=0.72$ ;  $x=0.78$  and  $x=0.90$ . In some cases, a platinum cylinder (5 mm in diameter) was also used as working electrode.

## Results

**Electrochemical characterizations.** Since the nickel ferrite electrodes are to be used as anodes during the electrowinning of aluminium, their behaviour was investigated at potentials comprised between their open-circuit potential (OCP) (1.40-1.50V/ref.) and the oxygen evolution potential (2.20 V/ref.). In a first step, the alumina-saturated cryolite melt was checked with a platinum electrode, which is considered as inert [13] and thus allows plotting a blank signal of the electrolyte. In a second step, the nickel ferrites were characterized in the same way and their behaviour was compared to platinum.

Linear voltammogram obtained on Pt is presented in Fig. 1. In addition of the oxygen evolution reaction that produces a strong current at potentials above  $E=2.20$  V/ref, a small residual current is observed in the 1.30-2.20 V/ref potential range. A potentiostatic electrolysis on Pt at  $E=1.95$  V/ref (Fig. 1) confirms the existence of this residual current (about  $15 \text{ mA/cm}^2$ ). The source of the reaction has not been established in this work, but it is believed from other experiments that it is linked to the presence of oxides in the melt.

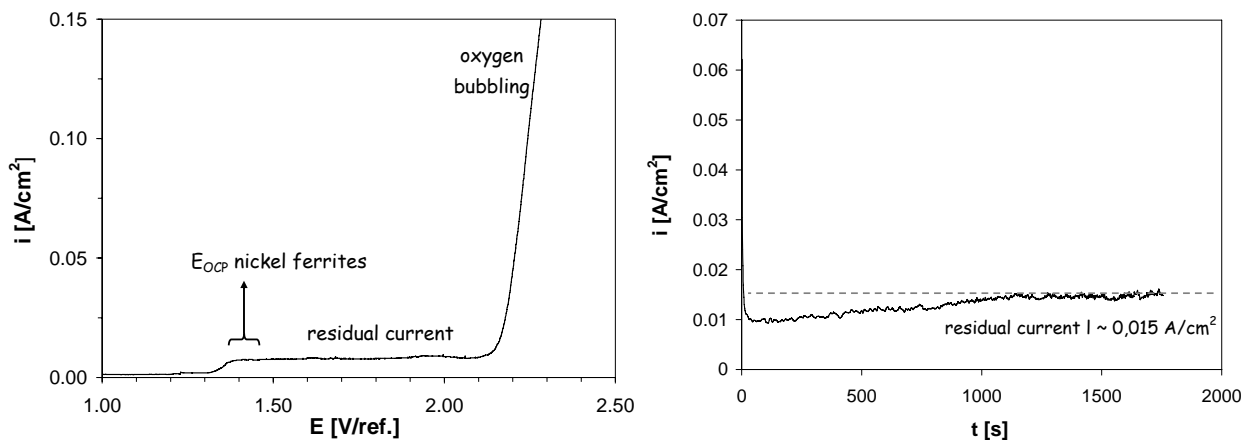


Fig.1: Linear voltammogram at  $s=10 \text{ mV/s}$  (left) and potentiostatic electrolysis at  $E=1.95\text{V/ref.}$  (right) on a platinum electrode in a cryolite melt ( $\text{CR}=2.2$ ;  $9\%\text{Al}_2\text{O}_3$ ;  $5\%\text{CaF}_2$ ) at  $960^\circ\text{C}$ .

Linear voltammograms plotted on nickel ferrites (Fig. 2) indicate a strong influence of their composition ( $x$ ). Ni-rich nickel ferrites ( $x=0.78$  and  $0.90$ ) exhibit roughly the same behaviour as the Pt electrode: a residual current is recorded before the oxygen evolution potential. For lower Ni contents ( $x=0$  and  $0.22$  and  $0.48$ ), a noticeable reaction takes place at potentials below the oxygen evolution, and the current density of the oxidation peak increases when the Ni content decreases.

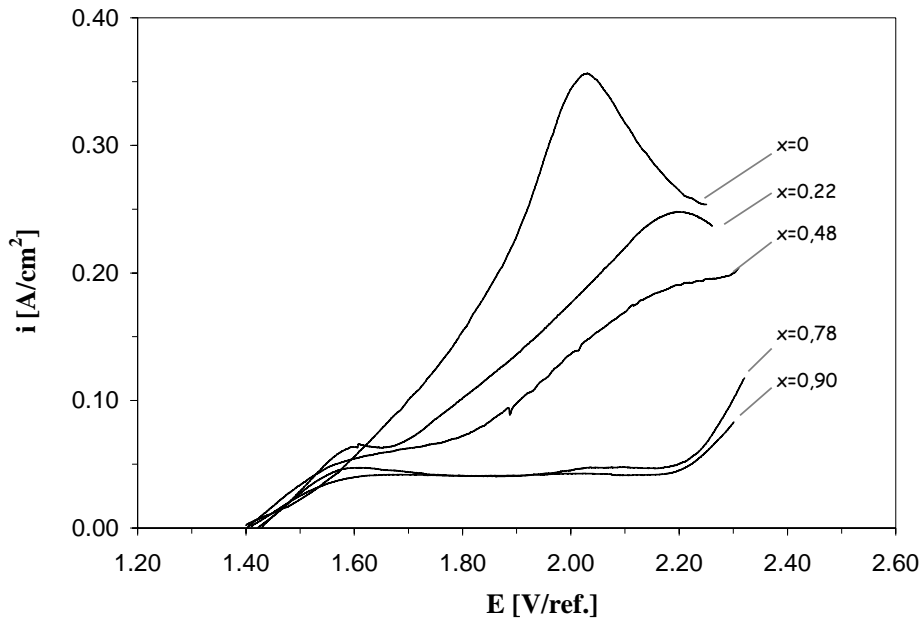


Fig.2: Linear voltammogram at  $s=10$  mV/s on nickel ferrites of various composition  $x$  ( $\text{Ni}_x\text{Fe}_{3-x}\text{O}_4$ ) in a cryolite melt (CR=2.2; 9% $\text{Al}_2\text{O}_3$ ; 5% $\text{CaF}_2$ ) at  $960^\circ\text{C}$ .

The influence of the composition of the nickel ferrites is further evidenced by potentiostatic electrolyses at  $E=1.95$  V/ref. (Fig. 3): the decrease of the current with time, which is typical of a diffusion-controlled process, becomes slower with the increase of the Ni content. The total charge applied during the electrolyses is plotted versus the Ni content in Fig. 3; the charge recorded on the Pt electrode is deducted in order to get rid of the influence of the residual current. This plot clearly confirms that the oxidation reaction is linked with the Ni content, as the total charge decrease from about  $43$  C/cm<sup>2</sup> for  $x=0$  to less than  $5$  C/cm<sup>2</sup> for  $x=0.90$ .

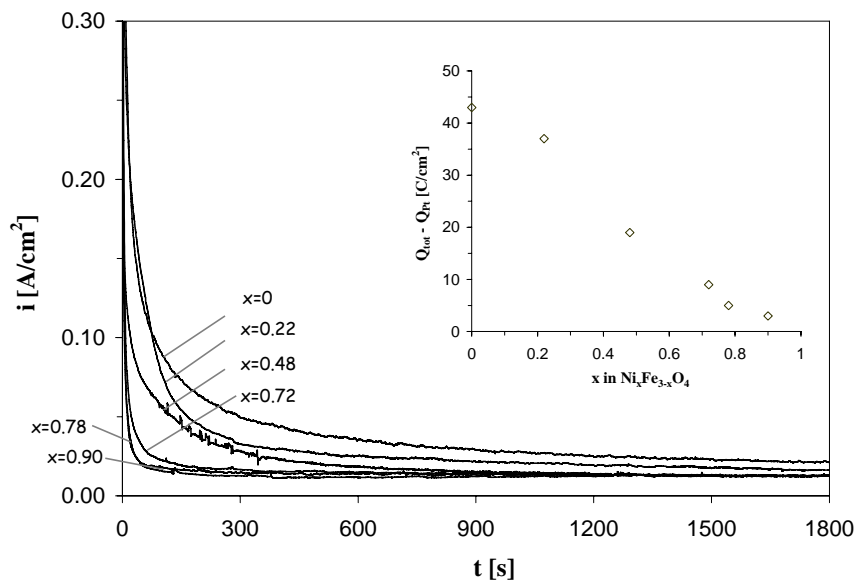


Fig.3: Evolution of the current density with time during potentiostatic electrolysis at  $E=1.95$  V/ref. on nickel ferrites of various composition  $x$  ( $\text{Ni}_x\text{Fe}_{3-x}\text{O}_4$ ) in a cryolite melt (CR=2.2; 9% $\text{Al}_2\text{O}_3$ ; 5% $\text{CaF}_2$ ) at  $960^\circ\text{C}$ .

**Ex situ material characterizations.** In order to understand the oxidation reaction evidenced by electrochemical measurements, the nickel ferrite electrodes were analysed after 30 minutes of polarization under three different conditions. Two electrolyses were performed at potential lower than the oxygen evolution potential ( $E=1.95$  V/ref and  $E=2.10$  V/ref) and one electrolysis was performed at constant current ( $i=0.5$  A/cm<sup>2</sup>), with oxygen evolution.

Optical and SEM characterizations of the cross section of the electrodes were performed after the electrolyses. As evidenced in Fig. 4 and Fig. 5, in some cases haematite ( $Fe_2O_3$ ) was formed in the outer part of the anodes, close to the interface with the molten salt, at the grain boundaries of the nickel ferrite. The amount of haematite was found to be higher for low Ni-content nickel ferrites (low  $x$ ). This corrosion reaction was not attributed to the presence of  $O_2(g)$  at the surface of the anode, since haematite formation was evidenced even after electrolysis at potential below the oxygen evolution potential.

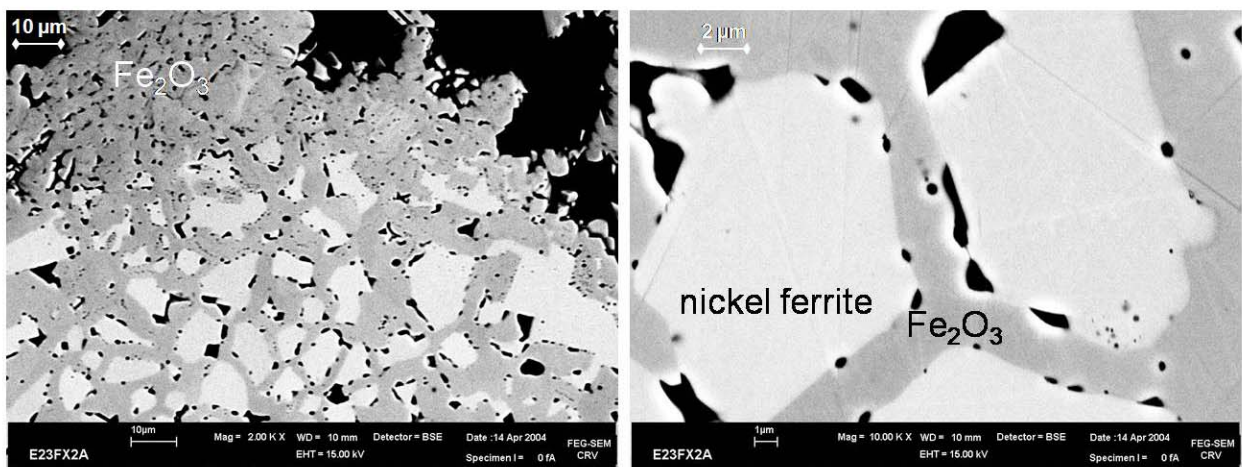


Fig. 4: Micrographs (SEM-BSE) of the cross section of a nickel ferrite ( $x=0.22$ ) after 30 minutes of polarization at  $E=1.95$  V/ref. in a cryolite melt ( $CR=2.2$ ;  $9\%Al_2O_3$ ;  $5\%CaF_2$ ) at  $960^\circ C$ . Grey phase: haematite; white phase: nickel ferrite.

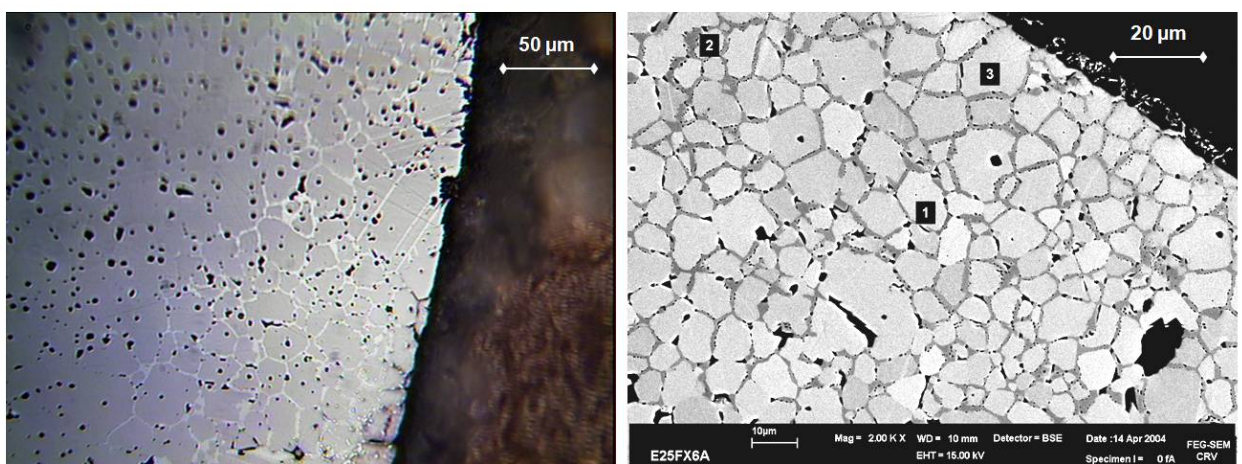


Fig. 5: Optical (left) and SEM (right) micrographs of the cross section of a nickel ferrite ( $x=0.72$ ) after 30 minutes of polarization at  $E=2.10$  V/ref. in a cryolite melt ( $CR=2.2$ ;  $9\%Al_2O_3$ ;  $5\%CaF_2$ ) at  $960^\circ C$ .

A summary of the characterization of the cross-sections of the anodes is presented in Table 1. These experimental results indicate that the haematite formation depends both on the electrolyses conditions (more anodic potentials favour the occurrence of haematite) and on the nickel ferrite composition (lower Ni content favour the occurrence of haematite). Among all the nickel ferrites that were studied, only one ( $x=0.90$ ) proved to be corrosion-resistant after 30 min of electrolysis under oxygen evolution.

Table 1: Detection (yes/no) of haematite in nickel ferrite electrodes after 30 min of electrolysis at three different potentials in a cryolite melt (CR=2.2; 9%Al<sub>2</sub>O<sub>3</sub>; 5%CaF<sub>2</sub>) at 960°C.

Composition x in Ni <sub>x</sub> Fe <sub>3-x</sub> O <sub>4</sub>	E=1.95 [V/ref.]	E=2.10 [V/ref.]	E>EO <sub>2</sub>
0	y	y	y
0.22	y	y	y
0.48	y	y	y
0.72	n	y	y
0.78	n	y	y
0.90	n	n	n

Concentration profiles were measured by microprobe analysis of the Fe and the Ni content in the centre of the grains composing the nickel ferrites, from the bulk of the electrodes to the surface. As shown in Fig. 6 in the case of a nickel ferrite with an initial composition  $x=0.48$  submitted to an electrolysis at  $i=0.5$  A/cm<sup>2</sup>, the Ni content was found to gradually increase at the proximity of the interface:  $x$  was equal to 0.48 (i.e. the bulk composition) at a distance of 500  $\mu$ m from the interface, and reached 0.92 on the surface of the anode. Similar concentration profiles were observed with other nickel ferrite compositions.

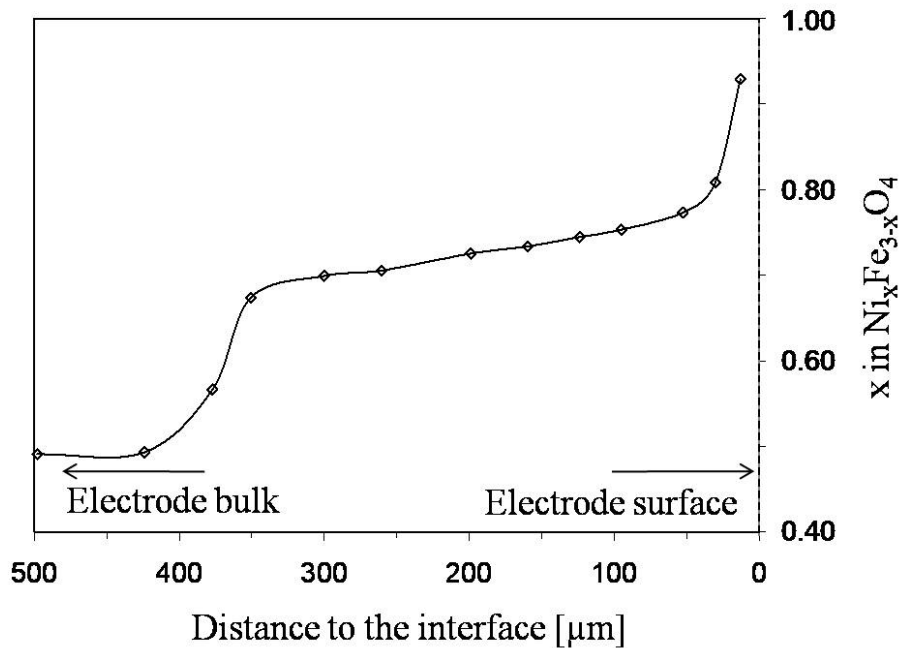


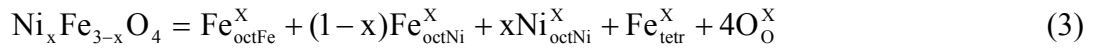
Fig. 6: Composition profile of a nickel ferrite ( $x=0.48$ ) after 30 minutes of polarization at  $i=0.5$  A/cm<sup>2</sup> in a cryolite melt (CR=2.2; 9%Al<sub>2</sub>O<sub>3</sub>; 5%CaF<sub>2</sub>) at 960°C.

## Discussion: oxidation mechanism of the nickel ferrites

A close understanding of the oxides constitution is necessary to comprehend the oxidation reaction. On the one hand, the nickel ferrites have a spinel structure with the following cationic distribution:



where *tetr* indicates tetrahedral sites and *oct* octahedral sites of the spinel structure. An increase of the Ni content  $x$  in the nickel ferrite leads to a proportional decrease of the  $\text{Fe}^{2+}$  content in the octahedral sites. Using the Kröger and Vink notation, the nickel ferrite structure can also be written as:



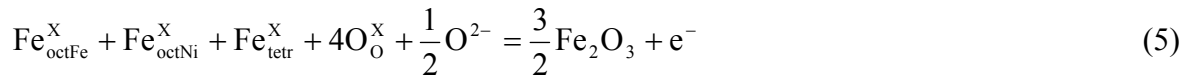
On the other hand, stoichiometric haematite is composed uniquely of  $\text{Fe}^{3+}$  cations:  $\text{Fe}^{3+}_2\text{O}^{2-}_3$ .

It is believed that the oxidation reaction evidenced by the experimental study is due to the oxidation of  $\text{Fe}^{2+}$  cations of the spinel phase into  $\text{Fe}^{3+}$  cations, which form the haematite phase. The simplified half-cell reaction is then:

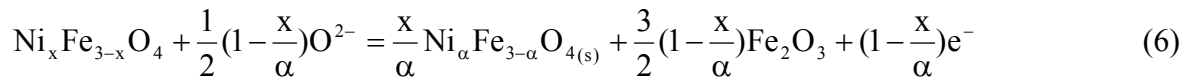


This reaction allows explaining why the intensity of the reaction measured by linear voltammetry is enhanced when  $x$  decreases: the amount of  $\text{Fe}^{2+}$  available in the spinel phase increases.

The disappearance of the ferrite lattice and the growth of the haematite is shown in Eq. (5) with the Kröger and Vink notation:



Taking into account the solid phases, Eq. (4) can also be written as:



with  $x < \alpha \leq 1$ .

Eq. (6) indicates that one mole of spinel (composition  $x$ ) in the bulk oxidises into  $x/\alpha$  moles of spinel (composition  $\alpha$ ) and  $3/2(1-x/\alpha)$  moles of  $\text{Fe}_2\text{O}_3$ . As a consequence, the total amount of spinel decreases, as well as the amount of Fe on the octahedral sites. This fits with the material characterization and especially with the concentration profiles (Fig. 6).

Eq. (5) and Eq. (6) also indicate that the formation of one mole of haematite requires  $1/3$  mole of  $\text{O}^{2-}$ , diffusing from the cryolite melt into the bulk of the anode. This anions transport explains how the oxidation of the anode is observed despite the absence of  $\text{O}_2(\text{g})$  evolution at the anode. Dissolved  $\text{O}^{2-}$  ions present in the melt (due to  $\text{Al}_2\text{O}_3$  dissolution) penetrate thus the nickel ferrite from the surface and participate in the formation of haematite.

## Conclusions

The characterisation of a wide range of composition of nickel ferrites used as anodes for the purpose of aluminium production was performed by electrochemical methods combined with SEM and microprobe analysis. It was shown that high Ni-content nickel ferrites are less subject to corrosion; these materials seem then to be better suited for a use as inert anode.

However, the electronic conductivity of the nickel ferrites is ensured by a  $\text{Fe}^{2+}/\text{Fe}^{3+}$  hopping mechanism: when the Ni content increases, the  $\text{Fe}^{2+}/\text{Fe}^{3+}$  ratio decreases, and so does the conductivity. As a consequence, high Ni-content nickel ferrites have a low conductivity (typically  $10 \text{ S/cm}^2$  for  $x=0.9$  at  $1000^\circ\text{C}$ ), which is not fully compatible with an industrial application, in spite of their satisfying behaviour against molten salts corrosion. Further research is then aiming at improving the electronic conductivity of such corrosion-resistant ceramic materials.

## Acknowledgments

This work was supported by Aluminium Pechiney and French “Ministère de l’Economie, des Finances et de l’Industrie”. The authors would like to thank V. Chastagnier (formerly at Pechiney CRV) for his support regarding microprobe analyses as well as S. Corso, P. Tailhades, I. Pasquet for the supply of the nickel ferrite electrodes. M. Pijolat and C. Honvault are also acknowledged for their help regarding the formalism of the oxidation mechanism.

## References

- [1] U.S. Department of Energy, *Technical Working Group on Inert anode Technologies*, Report of The American Society of Mechanical Engineers' (1999).
- [2] D.R. Sadoway: JOM Vol. 53-5 (2001), p. 34.
- [3] H. Xiao, *On the corrosion and the behavior of inert anodes in aluminum electrolysis*, PhD Thesis, NTNU, Trondheim (1993).
- [4] H. Alder, US Patent 3,930,967 (1976).
- [5] H. Wang, J. Yang, Y. Liu and J. Thonstad: T. Nonferr. Metal Soc. Vol. 2-4 (1992), p. 8.
- [6] A.D. McLeod, J.S. Haggerty and D.R. Sadoway: Light Metals (1986) p. 269.
- [7] A.D. McLeod, J.M. Lihman, J.S. Haggerty and D.R. Sadoway: Light Metals (1987) p. 357.
- [8] Y. Xianjin, Z. Lipeng and D. Yunhui: J. Rare Earth Vol. 24 (2006), p. 129.
- [9] R.A. DiMilia, J.M. Dynys, D.A. Weirauch, S.P. Ray, X. Liu and F.E. Phelps, US Patent 6,758,991 (2004).
- [10] S. Corso, P. Tailhades, I. Pasquet, A. Rousset, V. Laurent, A. Gabriel and C. Condolf: Solid State Sci. Vol. 6 (2004), p. 798.
- [11] A. Solheim, S. Rolseth, E. Skybakmoen, L. Stoen, A. Sterten and T. Store: Metall. Mater. Trans. B, Vol. 27B (1996), p. 744.
- [12] E. Skybakmoen, A. Solheim and A. Sterten: Metall. Mater. Trans. B, Vol. 28B (1997), p. 86.
- [13] J. Thonstad: Electrochim. Acta Vol. 13 (1968), p. 456.